In situ evaluation of interfacial affinity in CeO_2 based hybrid nanoparticles by pulsed field gradient NMR†

François Ribot,*[a] Virginie Escax,[b] Claire Roiland,[a] Clément Sanchez,[a] José C. Martins,[c] Monique Biesemans,[b] Ingrid Verbruggen[b] and Rudolph Willem[b]

Received (in Cambridge, UK) 29th July 2004, Accepted 25th November 2004
First published as an Advance Article on the web 4th January 2005
DOI: 10.1039/b411629a

Complexation affinity of laurate ligands ($C_{12}H_{23}O_2$) grafted onto the surface of cerium(IV) oxide nanoparticles can be probed and quantified *in situ*, by pulsed field gradient ^{1}H NMR through the dependence of the diffusion coefficient on the size of a species.

Because of their size related physical properties (quantum confinement, surface plasmon resonance, …) and their huge surface-to-volume ratio (catalysis, nanofillers, components of nanomembranes, …), nanoparticles represent a very important academic and technological research topic.[1] A fine understanding of their surface chemistry is needed since the adjustment of their size relies sometimes on the controlled poisoning of their growing surface by complexing ligands,[2] and their utilization often requires the functionalization of their surface, simply to avoid aggregation or to introduce new features such as hydrophobicity, protective shells, selective binding, optimized transferability into organic solvents or polymers.[3] The evaluation *in situ* of complexation affinities of organic ligands for inorganic nanoparticles is not an easy task. Yet, measuring this affinity is of paramount importance to gain a true control over the properties of hybrid organic–inorganic colloidal dispersions. Therefore, the availability of a convenient, fast and selective tool to probe and quantify the ligands bound to the surface of nanoparticles, with reference to the free ligands, is highly desirable. Pulsed field gradient (PFG) NMR offers such a tool by providing, in addition to chemical information through chemical shifts and scalar couplings, an elegant way to measure diffusion coefficients which, in turn, enable one to sort the species according to their size.[4] The use of PFG NMR is continuously expanding in bio-NMR, mixture analyses and polymer characterization.[5] It is also emerging as a powerful tool in organometallic chemistry.[6]

This work demonstrates that PFG ^{1}H NMR is also an efficient tool in the field of hybrid nanoparticles. It deals with probing and quantification of carboxylates at the surface of cerium(IV) oxide (CeO_2) nanoparticles. Such functionalized systems were recently used to elaborate porous materials with hierarchical structures.[7]

The cerium(IV) oxide nanoparticles used are spheroidal nanocrystals with a diameter of 3–4 nm as checked by XRD and TEM experiments.[7a] They can be readily dispersed in water, where they exhibit a hydrodynamic diameter of 6 nm (determined by quasi elastic light scattering), but cannot be dispersed in chloroform. On the contrary, the solid obtained after reaction with lauric acid is easily redispersed in organic solvents such as chloroform.‡ Its TEM observation (ESI)† indicates spheroidal nanoparticles of similar size.

The ^{1}H NMR spectrum in $CDCl_3$ of the solid obtained by reacting lauric acid with CeO_2 nanoparticles exhibits three well-resolved resonances (2.37, 1.66, and 0.90 ppm) for the α-CH_2, β-CH_2, and CH_3 moieties, respectively and a broader one (1.29 ppm) for all other CH_2 moieties (ESI). These four chemical shifts are identical to those observed for free lauric acid in $CDCl_3$. The system was studied by PFG ^{1}H NMR using a BPP-LED sequence.§[8] Fig. 1 shows the $\ln(I/I_0)$ against $(\gamma_H\delta g)^2(\Delta - \delta/3 - \tau/2)$ for each resonance (I: peak intensity for a given gradient strength, I_0: peak intensity for the minimum gradient strength, γ_H: proton gyromagnetic ratio, δ: gradient pulse length, g: gradient strength, Δ: diffusion time, and τ: time delay between the bipolar gradient pulse pair).

Except for the α-CH_2 group, the intensity of which is too weak at high gradient strength to be measured accurately, all the resonances show a fast and a slow attenuation regime, indicating the existence of two diffusion regimes for the lauryl groups.

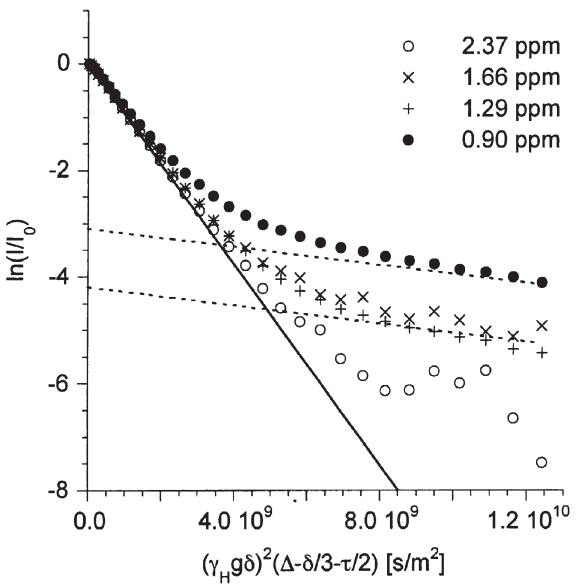

Fig. 1 Attenuation profiles for the resonances of lauric acid functionalized CeO_2 nanoparticles in $CDCl_3$ (the full and dotted lines show the linear attenuations calculated for $D = 9.4\ 10^{-10}$ and $8.5\ 10^{-11}$ $m^2\ s^{-1}$, respectively).

† Electronic supplementary information (ESI) available: TEM pictures and ^{1}H NMR spectrum of the functionalized nanoparticles. See http://www.rsc.org/suppdata/cc/b4/b411629a/

*fri@ccr.jussieu.fr

Accordingly, the intensity damping was fitted with the sum of two gaussians (eqn. (1)).

$$I/I_0 = (1 - x)\exp[-D_F(\gamma_H\delta g)^2\xi] + x\exp[-D_B(\gamma_H\delta g)^2\xi] \quad \text{with } \xi = \Delta - \delta/3 - \tau/2 \tag{1}$$

The results are reported in Table 1. The larger diffusion coefficient (D_F) compares well with the one of free lauric acid which, in the same solvent, shows a pure mono-gaussian attenuation profile associated with a diffusion coefficient of $8.9\ 10^{-10}\ m^2\ s^{-1}$.

According to the Stokes–Einstein formula and chloroform viscosity ($0.56\ 10^{-3}\ kg\ s^{-1}\ m^{-1}$ at 25 °C), the smaller value ($D_B \sim 8.5\ 10^{-11}\ m^2\ s^{-1}$) can be associated with species having a hydrodynamic diameter of ~ 9 nm, in good agreement with the hydrodynamic diameter of the CeO_2 nanoparticles prior to functionalization (6 nm). The main finding is that the PFG ^1H NMR clearly distinguishes the free ligands from those bound to the nanoparticles, even though a single chemical shift is found for each ^1H multiplet of the lauryl chains. Moreover, as two distinct diffusion coefficients are observed, the exchange rate between the free and bound ligands must be slow on the DOSY NMR time scale, its upper limit being estimated to be $\sim 8.3\ s^{-1}$ ($1/\Delta$). Fitting the attenuation profiles gives also access to the relative molar fractions of free and bound ligands. The results (Table 1) suggest these molar fractions to apparently depend on the resonance under investigation, the bound ligands being even not observed for the α-CH_2 group (2.37 ppm). This feature is most likely related to unavoidable T_2 decrease, as the associated rotational correlation time becoming increasingly long, parallels the methylene groups getting closer to the nanoparticle surface, tending to the value associated with the size of the particle ($\tau_c = 4\pi\eta r^3/3kT$).[9] Therefore, their signals get broader and contribute to a lesser extent to the intensity of the observed resonance that becomes increasingly dominated by the diffusional behaviour of the free ligands. The inability to quantify the diffusional behaviour of bound ligands through the α-CH_2 resonance can also be due to the fact that the resonance observed at 2.37 ppm is only related to the free ligands. The α-CH_2 resonance of the bound ligands could appear at higher frequency but should also flatten out into the spectrum noise because of the dramatically slower reorientational dynamics of the nanoparticles. Accordingly, the molar fraction determined for the most remote moiety, the methyl groups (0.90 ppm) is believed to be most relevant and reliable.

According to the overall sample composition (lauryl/Ce = 1.6), to the 5% of bound ligands and to the presence of about 40% of the cerium atoms on the surface of a spheroidal particle exhibiting a diameter of 3 nm and a cerium(IV) oxide structure, the ratio of the bound ligands to the surface cerium atoms is estimated to be *ca.* 20%. This coverage appears high enough to render the particles dispersible in chloroform.

Table 1 Diffusion coefficients, populations and residuals for each resonance

Chemical shift (ppm)	D_F ($m^2\ s^{-1}$)	x^a (%)	D_B ($m^2\ s^{-1}$)	ρ^b
0.90	$9.2\ 10^{-10}$	5	$9.2\ 10^{-11}$	$2.8\ 10^{-4}$
1.29	$9.4\ 10^{-10}$	2	$8.0\ 10^{-11}$	$2.0\ 10^{-4}$
1.66	$9.5\ 10^{-10}$	2	$8.2\ 10^{-11}$	$1.0\ 10^{-4}$
2.37	$9.4\ 10^{-10}$	0	—	$2.7\ 10^{-4}$

[a] Fraction of total ligand bound to CeO_2. [b] $\rho = \Sigma(Y_{obs} - Y_{cal})^2/\Sigma Y_{obs}^2$.

Additional work is underway to vary the overall carboxylic acid to cerium ratio in order to determine the full adsorption isotherm and the surface bonding constant.

Moreover, the work presented in this communication can be extended to many other non paramagnetic inorganic nanoparticles (SnO_2, TiO_2, ZrO_2, Al_2O_3, AlOOH, CdS, CdSe, …) complexed by a large variety of organic ligands (phosphonates, phosphine oxides, β-diketonates and analogues, α- or β-hydroxyacids, polyols, …). Therefore the present results have a strong and wide interest for the expanding community of scientists involved in nanoscience.

J.-Y. Chane Ching (Rhodia) is acknowledged for providing cerium(IV) oxide nanoparticles. R. W., M. B. and J. C. M. are indebted to the Fund for Scientific Research – Flanders (Belgium) (Grant G.0016.02), and to the Research Council of the VUB (Grants GOA31, OZR362, OZR875) for financial support. F. R. acknowledges the Fund for Scientific Research – Flanders (Belgium) (Grant FWOWO12) for financial support of several stays at the HNMR laboratory of the VUB. V. E. acknowledges a post-doctoral fellowship from the Fund for Scientific Research – Flanders.

François Ribot,*[a] Virginie Escax,[b] Claire Roiland,[a] Clément Sanchez,[a] José C. Martins,[c] Monique Biesemans,[b] Ingrid Verbruggen[b] and Rudolph Willem[b]

[a]*Chimie de la Matière Condensée (CNRS UMR 7574), Université Pierre et Marie Curie, 4 place Jussieu, Paris, 75252, France. E-mail: fri@ccr.jussieu.fr; Fax: 33 1 4427 4769; Tel: 33 1 4427 4135*

[b]*Hoog Resolutie NMR Centrum (HNMR), Vrije Universiteit Brussel, Pleinlaan 2, Brussel, 1050, Belgium*

[c]*Eenheid NMR en Structuuranalyse, Vakgroep Organische Chemie, Universiteit Gent, Krijgslaan 281, Gent, 9000, Belgium*

Notes and references

‡ The starting cerium oxide nanoparticles have the following composition $CeO_{1.8}(NO_3)_{0.4}\cdot(H_2O)_{1.1}$ according to the elemental analyses (found [calculated], Ce: 67.0% [65.6%], C: 0.0% [0.0%], N: 2.8% [2.6%], H: 1.1% [1.0%]). To be functionalized, they were dispersed in water (500 mg in 10 ml) and then reacted with lauric acid dispersed in warm water (60 °C) under vigorous magnetic stirring. A solid was recovered by centrifugation (10000 rpm for 10 min) and dried at 60 °C. According to elemental analyses, it corresponds to $CeO_{1.9}(NO_3)_{0.2}(H_{24}C_{12}O_2)_{1.6}$ (found [calculated], Ce: 28.0% [27.8%], C: 45.0% [45.8%], N: 0.7% [0.6%], H: 8.0% [7.7%]).

§ NMR: Pulsed field gradient NMR experiments were performed at 25 °C in $CDCl_3$ on a Bruker Avance 250 spectrometer with a BPP-LED (Bipolar Pulse Pair - Longitudinal Eddy current Delay) sequence (T_e = 5 ms, τ = 1 ms).[8] Diffusion time (Δ) and gradient pulse length (δ) were set to 60 and 3.2 ms, and 120 and 4 ms for lauric acid and functionalized nanoparticles, respectively. For each sample, 32 experiments were carried out with sine shaped gradient pulses ranging from 0.5 to 90% of the maximum gradient intensity (56 G/cm).

1 (*a*) *Nanomaterials: Synthesis, Properties and Applications*, ed. A. S. Edelstein, R. C. Cammarata, Institute of Physics, Bristol, 1996; (*b*) K. J. Klabunde and C. Mohs, in *Chemistry of Advanced Materials: an Overview*, ed. L. V. Interrante, M. J. Hampden-Smith, Wiley-VCH, New York, 1998, pp. 271–327; (*c*) C. Sanchez, G. J. A. A. Soler-Illia, F. Ribot, T. Lalot, C. R. Mayer and V. Cabuil, *Chem. Mater.*, 2001, **13**, 3061–3083.

2 (*a*) S. de Monredon, A. Cellot, F. Ribot, C. Sanchez, L. Armelao, L. Gueneau and L. Delattre, *J. Mater. Chem.*, 2002, **12**, 2396–2400; (*b*) M. A. Hines and P. Guyot-Sionnest, *J. Phys. Chem.*, 1996, **100**, 468–471; (*c*) J. Joo, T. Yu, W. Kim, H. M. Park, F. Wu, J. Z. Zhang and T. Hyeon,

J. Am. Chem. Soc., 2003, **125**, 6553–6557; (*d*) M. Brust, M. Walker, D. Bethell, D. J. Schiffrin and R. Whyman, *J. Chem. Soc., Chem. Commun.*, 1994, 801–802; (*e*) M. Niederberger, G. Garnweitner, F. Krumeich, R. Nesper, H. Cölfen and M. Antonietti, *Chem. Mater.*, 2004, **16**, 1202–1208.

3 (*a*) E. Bourgeat-Lami, *J. Nanosci. Nanotech.*, 2002, **2**, 1–24; (*b*) R. Shenhar and V. M. Rotello, *Acc. Chem. Res.*, 2003, **36**, 549–561; (*c*) R. Gref, P. Couvreur, G. Barratt and E. Mysiakine, *Biomaterials*, 2003, **24**, 4529–4537; (*d*) S. Roux, G. J. A. A. Soler-Illia, S. Desmoutier-Champagne, P. Audebert and C. Sanchez, *Adv. Mater.*, 2003, **15**, 217–221.

4 (*a*) E. O. Stejskal and J. E. Tanner, *J. Chem. Phys.*, 1965, **42**, 288–292; (*b*) C. S. Johnson, Jr, *Prog. Nucl. Magn. Reson. Spectrosc.*, 1999, **34**, 203–256.

5 (*a*) H. Barjat, G. A. Morris, S. Smart, A. G. Swanson and S. C. R. Williams, *J. Magn. Reson., Ser. B*, 1995, **108**, 170–172; (*b*) K. Bleicher, M. Lin, M. J. Shapiro and J. R. Wareing, *J. Org. Chem.*, 1998, **63**, 8486–8490; (*c*) B. J. Stockman and C. Dalvit, *Prog. Nucl. Magn. Reson. Spectrosc.*, 2002, **41**, 187–231; (*d*) B. Antalek, J. M. Hewitt, W. Windig, P. Yacobucci, T. Mourey and K. Le, *Magn. Reson. Chem.*, 2002, **40**, S60–S71; (*e*) T. Gostan, C. Moreau, A. Juteau, E. Guichard and M. A. Delsuc, *Magn. Reson. Chem.*, 2004, **42**, 496–499.

6 (*a*) M. Valentini, H. Rüegger and P. S. Pregosin, *Helv. Chim. Acta*, 2001, **84**, 2833–2853; (*b*) F. Ribot, V. Escax, J. C. Martins, M. Biesemans, L. Ghys, I. Verbruggen and R. Willem, *Chem. Eur. J.*, 2004, **10**, 1747–1751.

7 (*a*) A. Bouchara, G. Moser, G. J. A. A. Soler-Illia, J.-Y. Chane Ching and C. Sanchez, *J. Mater. Chem.*, 2004, **14**, 2347–2353; (*b*) A. Corma, P. Atienzar, H. Garcia and J.-Y. Chane-Ching, *Nat. Mater.*, 2004, **3**, 394–397.

8 D. Wu, A. Chen and C. S. Johnson, Jr., *J. Magn. Reson., Ser. A*, 1995, **115**, 260–264.

9 J. W. Akitt, *NMR and Chemistry: an Introduction to Modern NMR Spectroscopy*, 3rd edn., Chapman & Hall, London, 1992, p. 82.